

Evaluation of Non-contrast Dynamic MRA in Intracranial Arteriovenous Malformation (AVM): Comparison with time of flight (TOF) and digital subtraction angiography (DSA)

Songlin Yu¹, Lirong Yan², Yuqiang Yao³, Shuo Wang⁴, Mingqi Yang⁴, Bo Wang⁵, Yan Zhuo⁵, Lin Ai⁶, Xinyuan Miao⁵, Jizong Zhao⁴, and Danny J. J. Wang²

¹Beijing Tiantan Hospital, Capital Medical University, Beijing, China, People's Republic of, ²Department of Neurology University of California Los Angeles Ahmanson-Lovelace Brain Mapping Center, ³Beijing Jishuitan Hospital, Peking University, ⁴Beijing Tiantan Hospital, Capital Medical University, ⁵The State Key Laboratory of Brain and Cognitive Science, Institute of Biophysics, Chinese Academy of, ⁶Beijing Neurosurgical Institute

Introduction:

Digital subtraction angiography (DSA) remains the gold standard to diagnose intracranial arteriovenous malformations (AVMs) but is invasive. Existing MR angiography (MRA) is suboptimal for assessing the hemodynamics of AVMs and the use of contrast agent may not be suitable for patients with renal dysfunction. The objective of this study is to evaluate the clinical utility of a novel non-contrast 4D dynamic MRA (dMRA) [1] in the evaluation of intracranial AVMs, through comparison with DSA and time-of-flight (TOF) MRA.

Methods:

Nineteen patients (12 women, mean age 26.2 ± 10.7 years) with intracranial AVMs were examined with DSA, TOF and 4D dMRA respectively. DSA (4-vessel angiography) was performed on a biplane angiography system (Advantx LCV+, GE Healthcare, UK). All MR imaging were performed on a 3-T MR imager (Tim Trio; Siemens, Erlangen, Germany). Conventional MR sequences included axial T1-weighted 3D magnetization prepared rapid acquisition gradient-echo, and time-of-flight MR angiography (TR/TE=33/3.86 msec, spatial resolution= $0.57\text{mm} \times 0.57\text{mm} \times 0.65\text{mm}$). Dynamic MRA was implemented by combining pulsed arterial spin labeling with a segmented multiphase TrueFISP sequence [1]. Dynamic MRA was acquired by cardiac-gated and non-cardiac-gated acquisitions. For cardiac-gated acquisitions, a slab of 64 slices was acquired (TR=2.94ms, TE=TR/2, spatial resolution= $1\text{mm} \times 1\text{mm} \times 1\text{mm}$, flip angle=25). Depending on the cardiac cycle, 10-17 phases of dMRA images with a temporal resolution of 83ms were acquired within approximately 6 minutes. For non-cardiac-gated acquisitions, a slab of 20 slices with 2mm thickness was scanned (TR=4.16ms, TE=TR/2, spatial resolution= $0.9\text{mm} \times 0.9\text{mm} \times 2\text{mm}$, flip angle=25). Thirty phases of dMRA images with a temporal resolution of 83ms were acquired within approximately 7 minutes. Spetzler-Martin grading scale was evaluated using each of the above three methods independently by two raters. Diagnostic confidence scores for three components of AVMs (feeding artery, nidus and draining vein) were also rated. Kendall's coefficient of concordance was calculated to evaluate the reliability between two raters within each modality (dMRA, TOF, TOF plus dMRA). The Wilcoxon signed-rank test was applied to compare the diagnostic confidence scores between each pair of the three modalities.

Results:

Dynamic MRA was able to detect 16 out of all 19 AVMs (85%)(Fig. 1), and the ratings of AVM size and location completely matched those of DSA while TOF misclassified 3 cases. In particular, in a patient with history of hemorrhage (Fig. 2), dMRA was more accurate than TOF MRA which was confounded by the high signal intensity cause by methemoglobin. For the 3 negative cases on dMRA, 2 had low blood flow on DSA (received embolization treatments) and another had motion artifacts. When dMRA was combined with TOF MRA, significantly improved diagnostic ratings were achieved ($p<0.05$) compared to either technique alone. However, dMRA was only able to detect 5 out of 25 draining veins (20%) due to limit in the number of phases acquired (10-15) which was traded for $1\text{x}1\text{x}1\text{mm}^3$ spatial resolution using cardiac-gated acquisitions in the existing implementation.

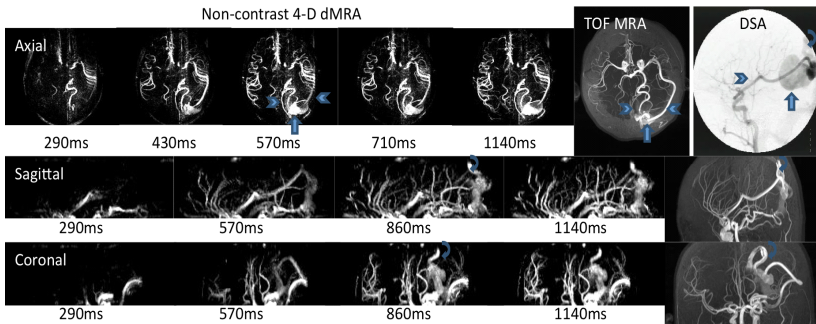


Fig. 1 DMRA images of an AVM in left occipital lobe. Consistent with TOF MRA and DSA, dMRA clearly revealed the dynamic courses for labeled blood from feeding arteries (MCA and PCA) (arrowheads), through abnormal vascular nidus (arrows) and then into the draining veins (curved arrows). Furthermore, dMRA revealed the heterogeneity within the nidus which was confirmed to be venous aneurysm but was unclear on TOF.

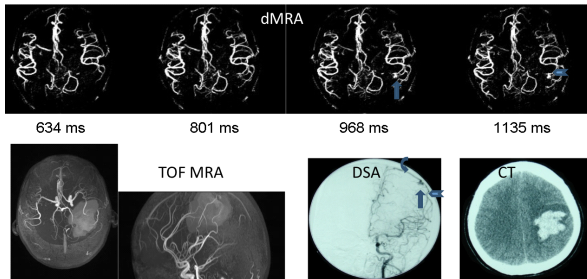


Fig. 2 Patient with spontaneous intracranial hemorrhage confirmed by CT. Axial dMRA shows a small AVM with a maximum diameter of 8mm with left MCA as its feeding artery. The draining vein was invisible due to the limit of acquisition window. This was confirmed by DSA. However, TOF failed to detect the AVM due to the disturbance of high signal intensity caused by methemoglobin and the size of the lesion was mistaken as enlarged (7cm).

Discussion:

Our results are consistent with a recent study comparing non-contrast dMRA with DSA in AVM patients [2]. Furthermore, we compared dMRA with TOF MRA. The hemodynamic information provided by dMRA improved diagnostic confidence scores by TOF MRA. As a completely noninvasive method, non-contrast 4D dMRA offers hemodynamic information with a temporal resolution of 50-100 milliseconds for the evaluation of AVMs, and can complement existing methods such as DSA and TOF MRA. Further development should be done to address its challenges for depicting draining veins of AVMs.

References: [1] Yan, L. et al., Radiology 256:270-9, 2010. [2] Xu, J. et al., JMRI 34:1199-205, 2011.